

Synergistic Effect of Exogeneous and Endogeneous Electrostimulation on Osteogenic Differentiation of Human Mesenchymal Stem Cells Seeded on Silk Scaffolds

Anıl S. Çakmak,^{1,2} Soner Çakmak,^{1,3} James D. White,¹ Waseem K. Raja,¹ Kyungsook Kim,¹ Sezin Yiğit,¹ David L. Kaplan,¹ Menemşe Gümüşderelioğlu^{2,3,4}

¹Department of Biomedical Engineering, Tufts University, 4 Colby Street, Medford 02155, Massachusetts, ²Bioengineering Division, Graduate School of Science and Engineering, Hacettepe University, Beytepe 06800, Ankara, Turkey, ³Nanotechnology and Nanomedicine Division, Graduate School of Science and Engineering, Hacettepe University, Beytepe 06800, Ankara, Turkey, ⁴Department of Chemical Engineering, Hacettepe University, Beytepe 06800, Ankara, Turkey

Received 7 April 2015; accepted 21 September 2015

Published online 7 October 2015 in Wiley Online Library (wileyonlinelibrary.com). DOI 10.1002/jor.23059

ABSTRACT: Bioelectrical regulation of bone fracture healing is important for many cellular events such as proliferation, migration, and differentiation. The aim of this study was to investigate the osteogenic differentiation potential of human mesenchymal stem cells (hMSCs) cultivated on silk scaffolds in response to different modes of electrostimulation (e.g., exogeneous and/or endogeneous). Endogeneous electrophysiology was altered through the use of monensin (10 nM) and glibenclamide (10 μ M), along with external electrostimulation (60 kHz; 100–500 mV). Monensin enhanced the expression of early osteogenic markers such as alkaline phosphatase (ALP) and runt-related transcription factor 2 (RUNX-2). When exogeneous electrostimulation was combined with glibenclamide, more mature osteogenic marker upregulation based on bone sialoprotein expression (BSP) and mineralization was found. These results suggest the potential to exploit both exogeneous and endogeneous biophysical control of cell functions towards tissue-specific goals. © 2015 Orthopaedic Research Society. Published by Wiley Periodicals, Inc. *J Orthop Res* 34:581–590, 2016.

Keywords: endogeneous electrostimulation; silk scaffolds; osteogenic differentiation; human mesenchymal stem cells

Bone regeneration is a biological process consisting of complex cell-mediated activities regulated by mechanobiological stimuli. In this process, differentiation of precursor cells to fibroblasts, chondrocytes, or osteoblasts is determined by biochemical and biophysical factors derived from the extracellular matrix (ECM) and interstitial fluids.¹ Various bioactive molecules such as cytokines and growth factors act as stimulants with time-dependent expression during bone formation.²

In contrast, biophysical stimulants, such as low intensity pulsed ultrasound (LIPU),³ pulsed electromagnetic fields (PEMF),⁴ low power direct current (DC),⁵ extracorporeal shockwave stimulation (ECSW),⁶ low intensity high frequency vibration (LIHFV),⁷ and low level laser therapy (LLLT)⁸ can impact bone regeneration. Electrical fields applied as direct current (DC) or alternative current (AC), are known regulators to guide development and regeneration of many tissues.⁹ AC devices supply bidirectional electrical fields and are classified as “capacitively coupled” (CC) and “inductively coupled” (IC). Clinically, electrical fields are used to enhance bone fracture healing via direct current (DC), capacitive (CC) or inductive coupling (IC) methods.^{10,11} DC methods have some disadvantages such as toxicity due to the electrodes, changes in pH, reduced levels of molecular oxygen, and the formation of Faradic products inside culture

media.¹² To avoid these problems, CC devices are preferred to obtain homogeneous electrical fields by using two parallel layers of noncorrosive platinum electrodes and electrical current can be transferred to ionic current at the electrode-electrolyte interface.^{13–15} Cell responses to electrical fields are connected with the calcium/calmodulin pathway resulting in an increase of intracellular Ca²⁺ content.¹⁶ DC and CC stimuli influence voltage-gated Ca²⁺ channels in the cell membrane and increase Ca²⁺ influx. In contrast, IC stimulation induces the release of Ca²⁺ from intracellular stores such as the endoplasmic reticulum.^{17,18} The elevated calcium level may alter downstream processes and elicit changes in the expression of genes involved in proliferation and differentiation.^{19,20}

The regenerative role of bioelectricity in bone, nerve, and muscle tissues has been studied.²¹ In bone, streaming potentials, currents, and piezoelectricity of collagen are related to bioelectricity.²² There have been many in vitro studies indicating changes in mRNA expression, protein synthesis, and differentiation in response to electrical fields. For example, enhanced alkaline phosphatase (ALP) and type I collagen expression, the upregulation of calcium mineralization and bone morphogenetic protein-2 (BMP-2) and -4 (BMP-4), transforming growth factor- β 1 (TGF- β 1), prostaglandin E and ECM deposition of decorin, osteocalcin, osteopontin, type I collagen, and type III collagen were observed in the presence of electrical fields.^{5,10,23–26}

For in vitro bone regeneration, beside the application of exogeneous electrical fields, electrostimulation was also generated using ion channel-targeting pharmacological agents to modulate the electrophysiological

Grant sponsor: NIH; Grant numbers: R01 AR061988, R01 AR005593

Correspondence to: Menemşe Gümüşderelioğlu (T: +90-312-297-7447; F: +90-312-299-2124; E-mail: menemse@hacettepe.edu.tr; menemse@gmail.com)

© 2015 Orthopaedic Research Society. Published by Wiley Periodicals, Inc.

properties of cells.²⁷ However, the combined effect of external electrostimulation and internal modulation of electrophysiology (membrane potential or V_{mem}) on the osteogenic differentiation of human mesenchymal stem cells (hMSCs) have not been reported.

The aim of this study was to investigate the synergistic effect of capacitively coupled electrical fields with endogeneously-applied electrostimulation on osteogenic differentiation of hMSCs seeded on silk scaffolds. Three dimensional (3-D) cultures with applied (exogeneous) electrical fields in the presence of monensin, an ionophore with selectivity for the Na^+ ions, and glibenclamide, an antagonist of the inward rectifying, ATP-sensitive K^+ channel (Kir6.x) were studied.

MATERIALS AND METHODS

Silk Scaffold Preparation

Aqueous solution of silk fibroin was obtained from *B. mori* silkworm cocoons (Tajima Shoji Co. LTD, Yokohama, Japan) according to previously reported methods.^{28,29} Then water-based silk scaffold fabrication was accomplished based on our prior study.²⁹ Four grams of granular NaCl particles (500–600 μ m in size) were added to 2 ml of 6% w/v silk solution in Teflon cylinders at room temperature. After 48 h, the containers were immersed in water to remove the salt particles from the scaffolds over 2 days by changing the water at least three times a day. The scaffolds were cut into discs (8 mm in diameter and 2 mm in thickness) and then, according to previously reported procedure³⁰ glycine-arginine-glycine-aspartic acid-serine (GRGDS) (Bachem, Torrance, CA) was coupled to scaffolds to improve cellular attachment. The scaffolds were sterilized in 70% ethanol for 30 min.

Electrostimulation System Design

Delrin[®] blocks, 30.5 × 30.5 cm, with a 1.25 cm thickness (McMaster Carr, Chicago, IL) were used to design electrostimulation chambers. Each block was divided into two sections and each section had two columns and five rows with holes suited to 35 mm cell culture Petri dishes (BD Biosciences, San Jose, CA). Two lines of holes for the wires, one around outside and one inside, were placed around the Petri dish holes in order to accomplish the electrical connections of the samples. With this design, 30 silk scaffolds could be stimulated concurrently.

The Petri dish design we have previously developed was used for the stimulation of cells seeded on the silk scaffolds.¹³ Briefly, two 2.5 cm long carbon rods (Electron Microscopy Sciences, Hatfield, PA) in 3 mm diameter were adhered in a Petri dish with an 8 mm distance using silicon glue. Each carbon rod was drilled from the opposite ends of the chamber and two 6 cm long platinum wires were linked to each carbon

rod separately in order to make electrical connections. Three scaffolds were tightly positioned between the carbon rods for the electrostimulation (Fig. 1). Frequency was applied at 60 kHz and voltage was varied in the range of 100–500 mV depending on the specific study.

A TENMA Universal Test Center 72-1005 Function Generator (TENMA Test Equipment, Springboro, OH) was used as a voltage source generating sinusoidal-wave electrical signals for all electrostimulation experiments. Applied voltage and frequency were confirmed using a Tektronix TDS 2024 Digital Oscilloscope (Tektronix, Beaverton, OR).

Cell Culture

Cell Seeding and Electrostimulation

Human mesenchymal stem cells (hMSCs) were isolated from bone marrow aspirate (Lonza, Gaithersburg, MD) as reported before.³¹ For cell seeding into the silk scaffolds, hMSCs were suspended in osteogenic differentiation medium with a cell density of 3×10^7 cells.ml⁻¹. Three silk scaffolds were placed tightly between carbon rods in Petri dishes and these Petri dishes were placed inside the electrostimulation chamber cavities. Control silk scaffolds (unstimulated) were also put inside 24-well cell culture dishes (Corning, Corning, NY). After 2 h conditioning in growth medium, 30 μ l cell suspension was added to the scaffolds and the same volume of medium was added every 30 min to prevent scaffolds from drying out. Petri dishes containing silk scaffolds were positioned in the electrostimulation chamber and connected to a copper wire via soldering. Each Petri dish was filled with 4.5 ml of osteogenic differentiation medium while each well in 24-well plates including control scaffolds were filled with 1.5 ml of medium. Electrostimulation was applied to the cells seeded on silk scaffolds for 1 h per day up to 28 days to observe the long term effect of electrostimulation. In this system, frequency was kept constant at 60 kHz and applied voltage was changed between 100 and 500 mV. Two different electrophysiology-modulating compounds, glibenclamide (Sigma, St. Louis, MO) and monensin (Abcam, Cambridge, MA), were used to treat the cells in the presence or absence of electrostimulation based on previous study.²⁷ These drugs were added to the osteogenic differentiation medium at 10 μ M glibenclamide and 10 nM monensin. Six experimental groups were included: (i) silk scaffolds; (ii) e-silk scaffolds; (iii) silk+mon scaffolds; (iv) e-silk+mon scaffolds; (v) silk+glib scaffolds; and (vi) e-silk+glib scaffolds. In this context, “e” is denoted for the samples that had applied electrical fields, “mon” and “glib” are denoted for samples that were cultured with monensin and glibenclamide, respectively. Silk scaffolds in the absence of electrical field were used as a control group.

Cell Proliferation

Alamar Blue assay was used for the evaluation of cell proliferation and viability. Seeded scaffolds in differentiation

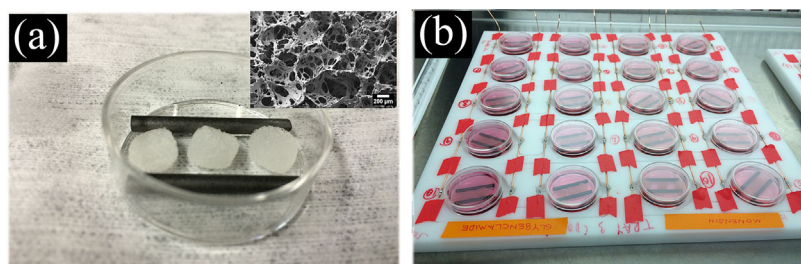


Figure 1. Electrostimulation system for silk scaffolds.

medium were incubated in culture medium supplemented with 10% (v/v) Alamar Blue reagent for 3 h at 37°C with 5% CO₂. Then, 200 µl of culture medium was transferred to a 96-well plate and fluorescence intensity was measured by a microplate reader (Spectramax Gemini XS, Molecular Devices) with an excitation wavelength of 550 nm and emission wavelength of 590 nm.

DNA Content and ALP Activity Analyses

Silk scaffolds were cut into two equal halves at days 7, 14, and 28 and washed in DPBS. One half was used to determine DNA content and ALP, while the other half was used for calcium analysis. DNA and ALP extraction were accomplished using initially CelLytic™ MT cell lysis reagent (Sigma–Aldrich, St. Louis, MO) and then, PicoGreen® assay (Life Technologies™, Grand Island, NY) and ALP assay kit (Abcam, Cambridge, MA) were used, respectively, according to the manufacturer's protocol at days 7, 14, and 28. DNA amount and ALP activity were normalized to gram of scaffold.

Calcium Content Analysis

The other half of the scaffold was washed in DPBS and placed in an Eppendorf tube, then 200 µl of ultrapure water was added to each sample. Scaffolds were placed into homogenizator with 10% amplitude for 30 s. Calcium was extracted by treating samples with 200 µl of 5% (v/v) trichloroacetic acid (Fisher Scientific, Pittsburgh, PA). The accumulated calcium was measured using a total calcium Liquicolor® kit (Stanbio, Boerne, TX) according to the manufacturer's protocol at days 7, 14, and 28. Calcium content was normalized to gram of scaffold.

Scanning Electron Microscope (SEM) Analysis

Morphology of the cells on scaffolds at days 7 and 28 were visualized by Zeiss Ultra-55 Field Emission Scanning Electron Microscope (Germany). After the culture medium was removed, samples were gently washed with DPBS (pH 7.4) twice and cells were fixed with 2.5% (v/v) glutaraldehyde in 0.1 M DPBS (pH 7.4) for 30 min at 4°C. Then, they were dehydrated in a series of ethanol (30%, 50%, 70%, 90%, and 100% v/v) and treated with hexamethyldisilazane (HMDS) before being dried. After the samples were completely dry, they were coated with a 5 nm gold layer prior to SEM analysis.

Real-Time RT-PCR Analysis

Scaffolds were first washed with DPBS before the analysis and transferred to new RNase, DNase free Eppendorf tubes. Two hundred microliter of Trizol (Life Technologies™, Grand Island, NY) was added to each Eppendorf tube and cell seeded samples were chopped with micro-scissors. Total RNA was extracted using RNeasy Mini kit (Qiagen, Valencia, CA) following the supplier's instructions and the RNA concentration was determined by measuring optical density at 260 nm using Nanodrop 2000 (Thermo Scientific, Wilmington, DE). cDNA was synthesized using a high-capacity cDNA kit (Applied Biosystems, Foster City, CA) and real time PCR was carried out with Taqman Gene Expression assay kit (Applied Biosystems) to detect transcript levels of runt-related transcription factor 2 (*RUNX-2*; Hs00231692_m1), collagen 1 alpha 1 (*COL1A1*; Hs00164004_m1), alkaline phosphatase (*ALP*; Hs01029144_m1), osteocalcin (*OCN*; Hs01587814_g1), bone sialoprotein (*BSP*; Hs00173720_m1), osteopontin (*OPN*; Hs00167093_m1), heat shock 70 kDa

protein 1B (*HSP70*; Hs00271244_s1), and heat shock 27 kDa protein 1 (*HSP27*; Hs00356629_g1). Expression levels of genes were quantified using a Stratagene MX30009 QPCR System (Stratagene, La Jolla, CA) and they were normalized to the housekeeping gene glyceraldehyde 3-phosphate dehydrogenase (*GAPDH*; Hs99999905_m1). Then, the data were expressed as fold change relative to silk scaffolds alone according to the first day of analysis using the $2^{-(\Delta\Delta Ct)}$ method.

Collagen Assay Analysis

The collagen content of silk, e-silk, silk+mon, and e-silk+mon groups were evaluated at day 14 and 28 to confirm *COL1A1* expression. Basically, samples were put to a new 24 well plate and washed two times with DPBS. They were kept inside an Eppendorf tube at -80°C until the analysis. To obtain cell lysates, 500 µl of pepsin solution (0.1 mg.ml⁻¹ in 0.5 M acetic acid) was added into each Eppendorf tube and tubes were incubated at 4°C overnight on a shaker. After digestion, lysate solution was transferred into a new Eppendorf tube and the amount of collagen was accomplished using Soluble Collagen Assay Kit (Sircol™, Northern Ireland, UK) according to the manufacturer's protocol.

Histology Analysis

Cell distribution within the scaffolds was visualized by histological staining of scaffold sections. Scaffolds were fixed in 4% (w/v) paraformaldehyde, embedded in paraffin, cut into 8 µm sections, and stained with hematoxylin and eosin for nuclei and cytoplasm. Mineral deposition was visualized by Alizarin Red and von Kossa stainings. All sections were evaluated with a Zeiss Axiovert S100 light microscope (Germany).

Statistical Analysis

All data were expressed as mean ± standard deviations of a representative of three parallel samples. Statistical analyses were performed with GraphPad InStat software (Graphpad Software, Inc., La Jolla, CA). One-way ANOVA was used to determine the significant differences among the groups and a statistical significance was assigned as **p* < 0.05, ***p* < 0.01, and ****p* < 0.001, respectively.

RESULTS AND DISCUSSION

3-D Electrostimulation System and Cell Culture Studies

Silk scaffolds (8 mm diameter, 2 mm thickness) obtained by salt leaching were used for the cultivation of hMSCs. The silk scaffolds had a high porosity of at least 90% with interconnected pores with a size distribution from 240 to 585 µm and average pore diameter of 416 ± 16 µm.

Electrical fields were applied via carbon rods and scaffolds were placed between two rods. The effect of electrical voltage on temperature and pH of the cell culture medium was checked during electrostimulation. Temperature increased no more than 1°C and pH did not change in the current electrical conditions. Before 3-D electrostimulation studies, preliminary studies were accomplished using platinum wire embedded silk films using different frequencies. High (60 kHz) and low (20 Hz) frequency electrical fields were applied to the hMSCs seeded silk films under 10 mV voltage. The results showed that 60 kHz

enhanced osteogenic differentiation of hMSCs according to *ALP*, *COL1A1*, and *BSP* expressions. Therefore, 60 kHz was chosen as an optimum frequency and an 8 mm electrode distance was determined to place scaffolds tightly between the rods. Different voltages, 100, 200, and 500 mV, were applied to the hMSCs seeded on the silk scaffolds and cell proliferation and gene expression were evaluated. There were no significant differences among the experimental groups based on the Alamar Blue results. On the other hand, the samples stimulated at 200 mV showed the highest *ALP* and *COL1A1* expression levels (data not shown). According to these results, 200 mV along with 60 kHz was determined as an optimum voltage for further 3-D electrostimulation studies and 100% duty cycle and 1 h duration per day was chosen from related studies in the literature.^{13,32–35} In addition to these external electrical fields, compounds that modulate internal membrane potential (monensin and glibenclamide) were added to the osteogenic medium.

Monensin is one of the most studied ionophores and forms complexes with sodium cations. It transports the complexed cation across cell membrane.³⁶ Glibenclamide is an anti-diabetic drug in a class of sulfonylureas and blocks ATP-sensitive potassium channels (K_{ATP}). This inhibition leads to increase intracellular calcium levels via opening voltage-dependent channels in the cell membrane.³⁷ Sundelacruz et al. quantified the effects of monensin and glibenclamide on membrane potential (V_{mem}) of hMSCs. DiSBAC, voltage-sensitive fluorescent dye, was used to measure relative changes in V_{mem} after treatment with drugs. Pharmacological treatments caused increases in fluorescence signals, which is indicative of depolarization of cell membrane.²⁷ It is known that bioelectrical signals play an important role in embryonic development and tissue regeneration. Bioelectrical signals are produced by ion currents according to cell membrane channels and pumps and ion transports regulate cell proliferation,

differentiation, and migration via generating pH and voltage gradients.^{27,38} In this study we aimed to generate endogenous bioelectrical signals via altering ion fluxes through the cell membrane to stimulate osteogenic differentiation of hMSCs by using ion channel-targeting agents, monensin and glibenclamide.

Cell Proliferation

Cell proliferation was evaluated with Alamar Blue analysis (Fig. 2a) and DNA content (Fig. 2b). Cell proliferation did not change during the culture in silk and e-silk groups ($p > 0.05$), although this was significantly higher in silk+mon ($p < 0.05$) and silk+glib ($p < 0.01$) groups from day 14 to day 28. Statistical analysis indicated low cell proliferation in e-silk and e-silk+mon groups compared to the control group at day 28 ($p < 0.001$). Furthermore, treatment of monensin and glibenclamide increased cell proliferation with respect to all electrically stimulated groups ($p < 0.001$). Under the electrical fields, glibenclamide supplemented medium resulted in a higher level of cell proliferation ($p < 0.001$) at day 28 (follow the arrow in Fig. 2). These data were confirmed by DNA analysis. Similarly, the silk+mon group showed the highest cell proliferation compared to the e-silk ($p < 0.01$), e-silk+mon ($p < 0.01$), silk+glib ($p < 0.01$), and e-silk+glib ($p < 0.05$) groups at day 28. According to these data, electrical fields decreased cell proliferation slightly in the silk and silk+mon groups, while it did not change in glibenclamide treated samples for both stimulated or unstimulated groups.

Cell Differentiation

ALP Activity

ALP activity is an early marker for osteogenic differentiation, moreover it plays a critical role in initiation of matrix mineralization.³⁹ As shown in Figure 3a. ALP activity was maintained at a constant level for the whole culture time in the silk ($p > 0.05$). ALP activity

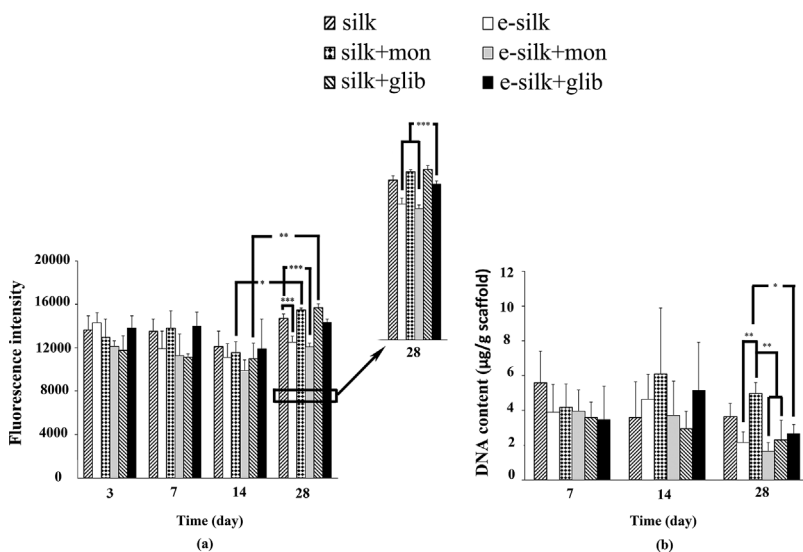


Figure 2. (a) Cell proliferation and (b) DNA content of hMSCs seeded on silk scaffolds in 3-D electrostimulation systems. Electrostimulation studies were carried out at 60 kHz and 200 mV. The results are represented as the mean \pm standard deviation for $n = 3$. Statistically significant differences are denoted by symbols; * $p < 0.05$, ** $p < 0.01$, and *** $p < 0.001$.

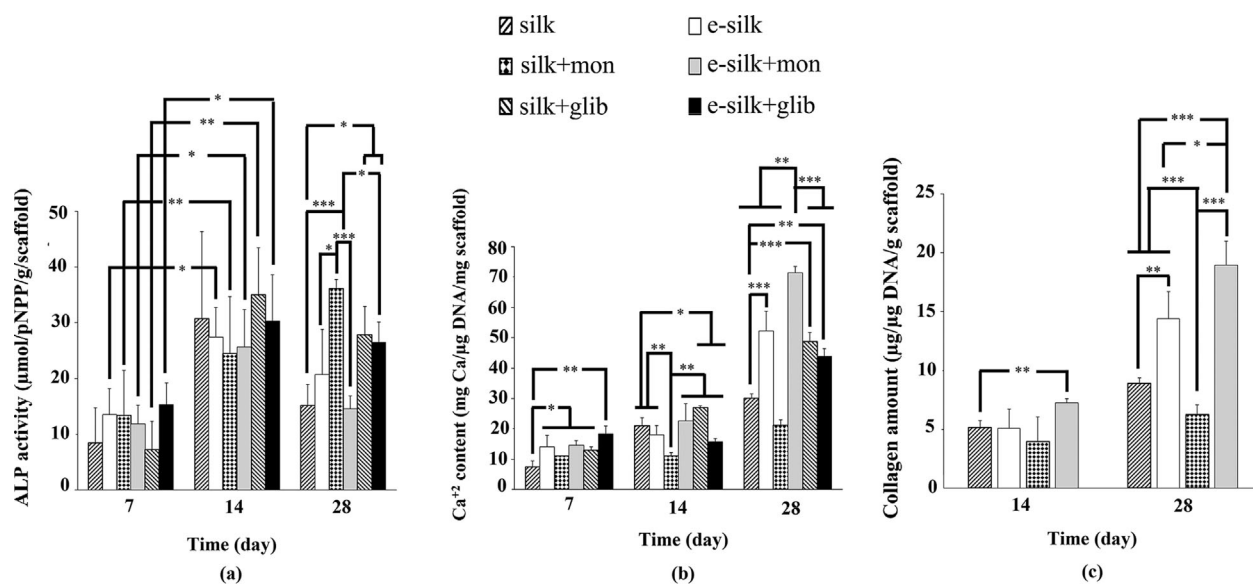


Figure 3. (a) ALP activity, (b) calcium analyses, and (c) collagen assay of hMSCs seeded on silk scaffolds in 3-D electrostimulation systems. Electrostimulation studies were carried out at 60 kHz and 200 mV. The results are represented as the mean \pm standard deviation for $n = 3$. Statistically significant differences are denoted by symbols; * $p < 0.05$, ** $p < 0.01$ and *** $p < 0.001$.

showed a further increase up to 2 weeks in the e-silk ($p < 0.05$), silk+mon ($p < 0.01$), e-silk+mon ($p < 0.05$), silk+glib ($p < 0.01$), and e-silk+glib ($p < 0.05$) groups and significantly greater activity was observed in the silk+mon group compared to the control ($p < 0.001$), e-silk ($p < 0.05$), and e-silk+glib ($p < 0.05$) groups at day 28. At the same time, electrical fields reduced ALP activity in the monensin treated groups at day 28 ($p < 0.001$). Also, the silk+glib and e-silk+glib groups exhibited significantly higher ALP levels than the control group at day 28 ($p < 0.05$).

Calcium (Ca²⁺) Content

Ca²⁺ presence is a late stage marker of osteogenic differentiation.⁴⁰ All groups showed an increase in calcium content over time and electrical fields enhanced Ca²⁺ content in all groups with respect to the control group at day 7 (Fig. 3b). The silk+mon group showed the lowest Ca²⁺ content compared to all groups at days 14 and 28 ($p < 0.01$). On the other hand, the electrical field in the monensin treated group stimulated Ca²⁺ content and reached significantly higher levels than the other groups ($p < 0.001$) at day 28. Glibenclamide increased Ca²⁺ content with or without an electrical field at day 14 ($p < 0.05$). Also, the e-silk ($p < 0.001$), silk+glib ($p < 0.001$), and e-silk+glib ($p < 0.01$) groups showed significantly higher calcium deposition than that of the control group at day 28.

RT-PCR Analysis

We analyzed the expression of key mRNA markers to examine osteogenic differentiation (Fig. 4). Electrostimulation with electrical field and electrophysiological modulating compounds did not have a statistically significant effect on early- and mid-stage osteogenic

differentiation markers (*RUNX-2*, *ALP*, *COLL1A1*) at day 7. *RUNX-2* expression increased in the silk+mon samples compared to all other groups at day 14 ($p < 0.01$). At day 28, *RUNX-2* expression increased in the e-silk+mon group and showed a similar profile to the silk+mon samples (Fig. 4a). *RUNX-2* is a transcription factor essential for osteogenesis, leading expression of other osteogenic genes.⁴¹ *ALP* expression in the scaffolds showed a similar trend with *RUNX-2* expression. The silk+mon samples had a statistically higher *ALP* upregulation than the other groups at the end of the 4th week of culture ($p < 0.001$). *ALP* expression increased in the e-silk+mon samples at day 28 ($p < 0.001$) (Fig. 4b). There was no significant difference in glibenclamide treated groups compared to the control group based on *RUNX-2* or *ALP* expression. *COLL1A1* expression did not change during the cultivation in all groups except the silk+mon samples (Fig. 4c). Monensin reduced *COLL1A1* expression at day 28 ($p < 0.001$). On the other hand, the electrical field maintained *COLL1A1* expression at a certain level in the monensin treated group. Collagen assay confirmed *COLL1A1* expression. The electrical field significantly stimulated collagen content in the e-silk+mon group compared to only monensin treated samples (Fig. 3c). Furthermore, the silk+glib ($p < 0.001$) and e-silk+glib ($p < 0.001$) samples had significantly higher *COLL1A1* expression levels than the silk+mon group. Upregulated *COLL1A1* expression was found in the e-silk+glib samples compared to the control group at day 28 ($p < 0.05$).

Bone sialoprotein (BSP) and osteopontin (OPN) expressions were examined to evaluate late stage osteogenic differentiation (Fig. 4d,e). Glibenclamide treated samples showed enhanced *BSP* expression at days 7 and 14 ($p < 0.001$). At day 14, e-silk+glib group enhanced the *BSP* expression compared to other groups except

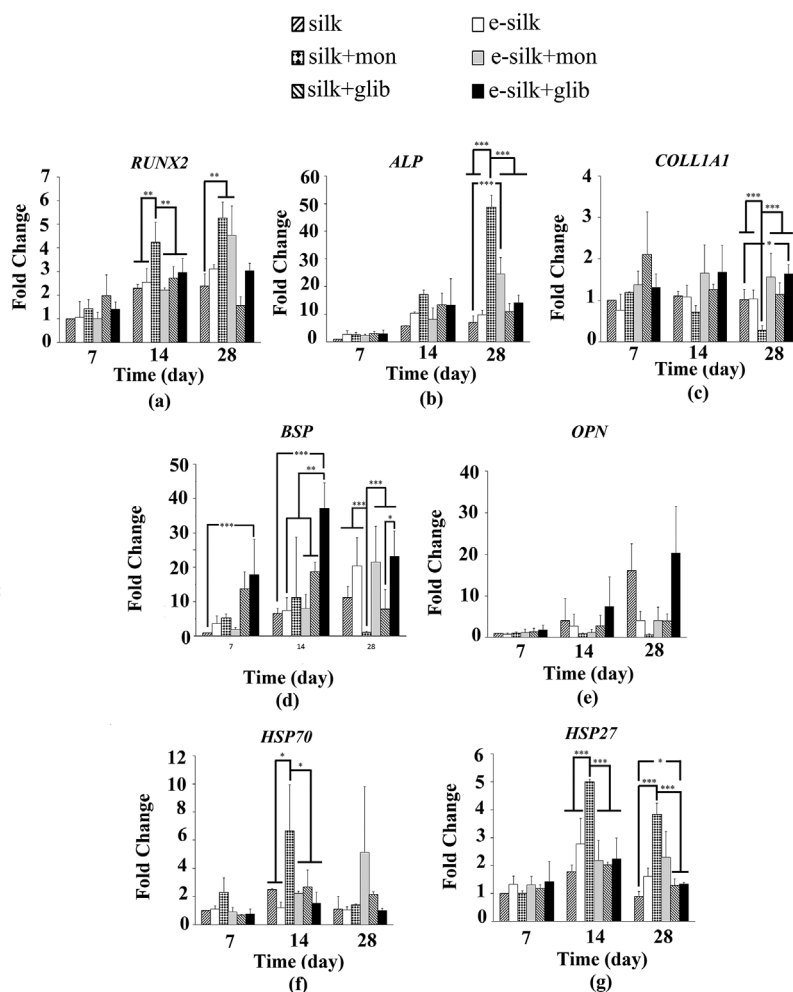


Figure 4. Quantitative RT-PCR analyses of (a) *RUNX-2*, (b) *ALP*, (c) *COLLI1A1*, (d) *BSP*, (e) *OPN*, (f) *HSP70*, and (g) *HSP27* genes. Electrostimulation studies were carried out at 60 kHz and 200 mV. The results are represented as the mean \pm standard deviation for $n = 3$. Statistically significant differences are denoted by symbols; * $p < 0.05$, ** $p < 0.01$ and *** $p < 0.001$.

silk+mon group. Also e-silk+glib group had quantitatively higher *BSP* expression level than silk+mon group, but this difference is not statistically significant. Besides, glibenclamide treated samples showed increased *BSP* expression under the electrical field with respect to silk+glib in a result of synergistic effect of glibenclamide and electrical field ($p < 0.01$). The silk+mon group showed significantly lower *BSP* expression compared to the other groups at day 28 ($p < 0.001$), however, the electrical field elevated *BSP* expression in this group with respect to the only monensin treated group ($p < 0.001$). Also, glibenclamide under the electrical field resulted in higher *BSP* expression compared to the only glibenclamide treated group at day 28 ($p < 0.05$). According to *OPN* expression, there was no significant difference between the groups at days 7 and 14. On the other hand, *OPN* expression showed constant profile in all samples except the control and e-silk+glib groups from days 14 to 28. However, there was no statistically significant difference in these samples.

Heat shock proteins, HSP70 and HSP27, were studied within the context of RT-PCR analysis (Fig. 4f,g). Heat shock proteins are upregulated under stress conditions such as oxidative damage and increased temperature to provide cellular homeostasis by modulating protein folding, degradation, and secretion.¹⁰ Furthermore,

cellular differentiation responses can be influenced by heat shock proteins.^{42,43} In the present study, no differences with respect to heat shock proteins were found among the groups at day 7 ($p > 0.05$). At day 14, the silk+mon group showed elevated expression level for both genes, *HSP27* ($p < 0.001$) and *HSP70* ($p < 0.05$) with respect to other groups. *HSP70* expression decreased in the silk+mon group at day 28, while *HSP27* expression remained at a constant level. Moreover, the electrical fields stimulated *HSP27* expression in the monensin treated samples compared to the control group at day 28 ($p < 0.001$). *HSP27* expression also increased in the e-silk+glib samples compared to the control group ($p < 0.05$).

Evaluation of gene expression of the scaffolds indicated that only electrical fields increased *ALP* expression, however, there were no significant differences among the other genes. Also Ca^{2+} content was enhanced under the electrical field. Monensin treatment promoted early stage osteogenesis based on *RUNX-2* and *ALP* expression. *ALP* activity confirmed this data, since the silk+mon samples had enhanced *ALP* activity with respect to the other groups. Furthermore, *HSP27* and *HSP70* expression were significantly higher in the silk+mon samples and exhibited similar profiles with *ALP* expression. In prior studies, *ALP* activity was

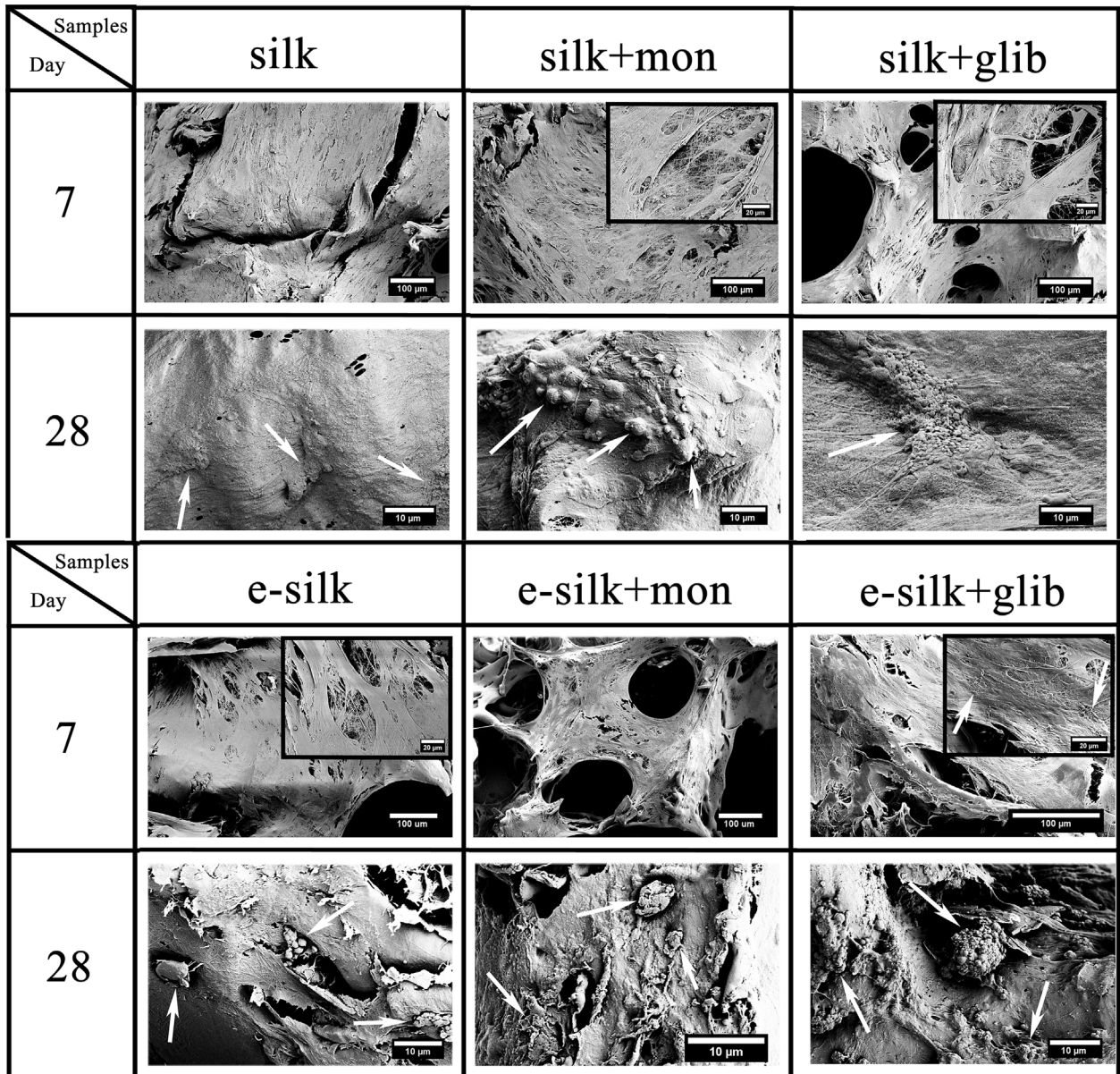


Figure 5. SEM images of hMSCs on silk scaffolds at days 7 and 28. Arrows indicate the mineralization spots.

induced by heat shock proteins in human bone marrow stromal cells.⁴⁴ Heat shock protein expression was regulated by a transcription factor known as heat shock factor (HSF). In normal cells, HSF is in a monomeric form in both the cytoplasm and nucleus and has no DNA binding activity. In stress conditions, HSF changes to a trimeric form and accumulates in the nucleus, then binding to DNA recognition sites and to facilitate transcription of heat shock proteins.⁴⁵ Monensin is a Na^+ specific ionophore and induces the depolarization of the cell membrane.²⁷ Enhanced expression of heat shock proteins indicated that alteration of intracellular Na^+ content and cell membrane potential may be a physiological stress in cells in the silk+mon samples and the upregulation of heat shock genes improved early stage osteogenic differentiation.

On the other side, Ca^{+2} content and the expression of mineralization-related genes, *BSP* and *OPN*, were lower in the monensin treated samples. Also, *COLL1A1* expression decreased in the silk+mon samples at day 28. Monensin induces intracellular accumulation of secreted components and also results in a lack of extracellular fiber formation by blocking protein transport through the Golgi apparatus.⁴⁶ Low collagen expression levels may be related to inhibition of protein transport by monensin in the silk+mon samples. However, electrical fields eliminated the negative effect of monensin on *BSP*, *OPN*, and *COLL1A1* expressions and resulted in the significant upregulation of these genes compared to the silk+mon group. Electrical fields may affect osteogenic differentiation through elevated intracellular Ca^{2+} levels and signaling pathways.

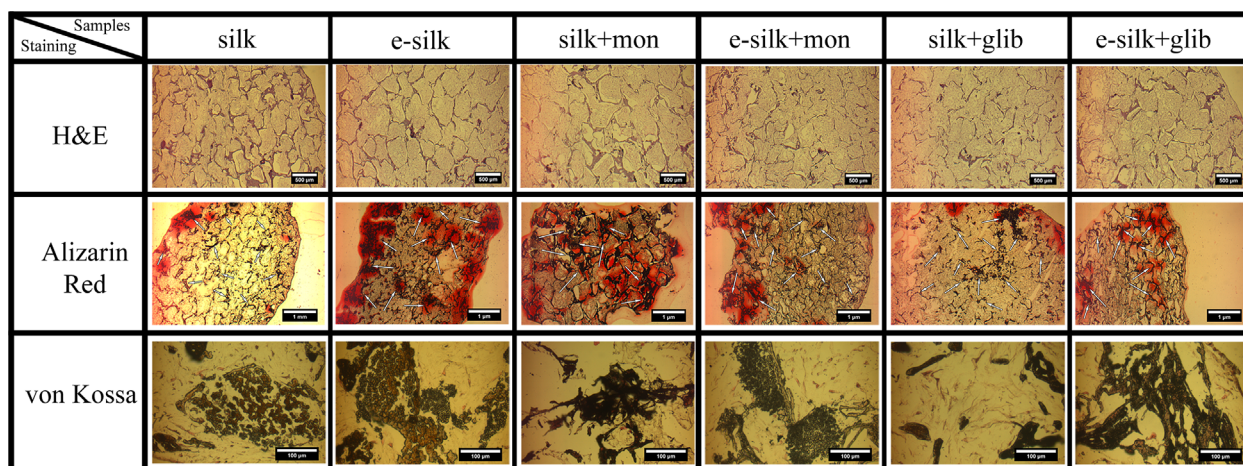


Figure 6. H&E, Alizarin Red, and von Kossa stainings of silk scaffolds at day 28. Dark purple color in H&E staining sections indicate pore walls of silk scaffolds and light purple color shows cell distributions inside the pores. Brownish-black colors in Alizarin Red and von Kossa stainings indicate calcium rich mineralized areas and arrows indicate the mineralization spots. In each image, left and right columns present low and high magnifications, respectively.

On the other hand, glibenclamide treated samples showed increased Ca^{2+} content and *BSP* expression. Glibenclamide blocks ATP-dependent K^+ channels and the role of these channels is closely linked to extracellular Ca^{2+} concentration by opening voltage-activated Ca^{2+} channels.⁴⁷ Osteoblast-like cells treated with glibenclamide increased osteocalcin synthesis via Ca^{2+} channels.⁴⁷ Glibenclamide is thought to be effective on mineralization via adenosine triphosphate (ATP). ATP is a type of extracellular signalling molecule besides a mediator of cellular activities. Previous studies have shown that exogenous ATP inhibits mineralization of the collagenous matrix. Two mechanisms are responsible for this effect; P2 receptor-dependent pathways and receptor-independent mechanisms. In the second mechanism, the mineralization inhibitor pyrophosphate, PPI, forms as a result of the hydrolysis of ATP.^{48,49} Glibenclamide restricts extracellular ATP levels by blocking ATP-dependent K^+ channels and suppresses the negative effect of ATP on mineralization. We conclude that glibenclamide and electrical fields provide a synergistic effect on cells by promoting mineralization and stimulating osteogenic differentiation.

Cellular Morphology

SEM images showed that cells attached and spread in the scaffolds in all groups at days 7 and 28 (Fig. 5). More specifically, hMSCs in all groups produced high amount of ECM indicated by collagenous structure at day 7. Scaffolds were covered with overlying cell layers and collagenous matrix in e-silk or monensin and glibenclamide systems (inset images). Some mineralization spots were observed on the collagen fibers in the e-silk+glib samples (inset image). The scaffold surfaces were almost completely covered by multiple layers of cells and/or new ECM under the electrical field at day 28. Cells filled the spaces inside and between the pores in the presence of electrical stimulation (Fig. S1). Electrical field increased the size of

nodules as evidence of mineralized matrices in all samples compared to unstimulated groups. However, cluster of apatite-like crystals as big as $10\ \mu\text{m}$ size were observed in glibenclamide samples in the presence of electrostimulation. Globular nodule structures in these samples are similar to mineralization during osteogenesis as the nodules are mineralized matrix vesicles and are considered as precursors of mineral spherules which represent the sites of new mineral formation and stimulate biomineralization.⁵⁰ SEM images confirmed elevated mineralization-related gene expression such as *BSP* and *OPN* in the e-silk+glib samples.

Histological Evaluation

H&E staining of scaffolds indicated that cell distribution and content within the scaffold was dense and uniform in all groups at day 28 (Fig. 6). Interconnected pore structures facilitated migration of cells inside the scaffolds. Alizarin Red and von Kossa stainings indicated mineral deposition in samples (Fig. 6). Microscopic observation showed more homogenous and central mineralization in e-silk, silk+mon, and e-silk+glib groups with respect to the control group. On the other hand, although mineralization increased in e-silk+mon and silk+glib groups compared to control group, the presence of calcium minerals were not uniform. In the control group, stained areas were only close to the edges of the scaffolds. Also, mineral deposition in large areas was confirmed by Alizarin Red and von Kossa assays in the e-silk+glib samples.

All analysis for mineralization, *BSP*, and *OPN* expressions, Alizarin Red and von Kossa stainings, suggested the stimulation of osteogenic differentiation in the e-silk+glib samples. In a similar way, glibenclamide showed a synergistic effect with electrical field on osteogenic differentiation of hMSCs via Ca^{2+} ions. Histological evaluation confirmed the RT-PCR results and SEM images.

CONCLUSIONS

We exposed CC electrical fields to hMSCs cultivated on silk scaffolds in the presence of electrophysiology modulating compounds, monensin and glibenclamide, which are effective on voltage-gated channels in the cell membrane. Both compounds had distinct effects on cell behaviour under electrical fields: (i) monensin treatment promoted early stage osteogenesis based on *RUNX-2* and *ALP* expression and also enhanced the expression of heat shock proteins, *HSP27*, *HSP70*; (ii) monensin reduced *BSP*, *OPN*, and *COLL1A1* expression, however, electrical fields eliminated the negative effects of monensin; and (iii) glibenclamide had a synergistic effect with electrical field and enhanced osteogenic differentiation indicated by *BSP* expression and mineralization. Electrical fields and ion channel-targeting pharmacological agents can be used as alternatives to mechanical stimulation and growth factors in regulation cell and tissue outcomes.

AUTHORS' CONTRIBUTIONS

A.S.Ç. and S.Ç. designed and performed the experiments, collected and analysed the data. J.D.W. and W.K.R. contributed to the design of electrostimulation system. K.K. performed the collagen assay experiments. S.Y. contributed to the electrostimulation application. A.S.Ç., D.L.Kaplan and M.G. prepared the manuscript. All authors read and approved the final submitted manuscript.

ACKNOWLEDGMENTS

Anil S. Çakmak thanks The Scientific and Technological Research Council of Turkey (TUBITAK) for providing an International Research Fellowship. Soner Çakmak was supported by the Hacettepe University, Scientific Research Projects Coordination Unit, BAB 6091–International Scientific Cooperation Development Support.

REFERENCES

- Lacroix D, Prendergast PJ, Li G, et al. 2002. Biomechanical model to simulate tissue differentiation and bone regeneration: application to fracture healing. *Med Biol Eng Comput* 40:14–21.
- Wiesmann HP, Joos U, Meyer U. 2004. Biological and biophysical principles in extracorporeal bone tissue engineering. Part II. *Int J Oral Maxillofac Surg* 33:523–530.
- Yang KH, Parvizi J, Wang SJ, et al. 1996. Exposure to low-intensity ultrasound increases aggrecan gene expression in a rat femur fracture model. *J Orthop Res* 14:802–809.
- Tsai MT, Li WJ, Tuan RS, et al. 2009. Modulation of osteogenesis in human mesenchymal stem cells by specific pulsed electromagnetic field stimulation. *J Orthop Res* 27:1169–1174.
- Sun S, Liu Y, Lipsky S, et al. 2007. Physical manipulation of calcium oscillations facilitates osteodifferentiation of human mesenchymal stem cells. *FASEB J* 21:1472–1480.
- Wang CJ, Liu HC, Fu TH. 2007. The effects of extracorporeal shockwave on acute high-energy long bone fractures of the lower extremity. *Arch Orthop Trauma Surg* 127:137–142.
- Srinivasan S, Weimer DA, Agans SC, et al. 2002. Low-magnitude mechanical loading becomes osteogenic when rest is inserted between each load cycle. *J Bone and Miner Res* 17:1613–1620.
- Stein A, Benayahu D, Maltz L, et al. 2005. Low-level laser irradiation promotes proliferation and differentiation of human osteoblasts in vitro. *Photomed Laser Surg* 23:161–166.
- Levin M, Stevenson CG. 2012. Regulation of cell behavior and tissue patterning by bioelectrical signals: challenges and opportunities for biomedical engineering. *Annu Rev Biomed Eng* 14:295–323.
- Hronik-Tupaj M, Kaplan DL. 2012. A review of the responses of two- and three-dimensional engineered tissues to electric fields. *Tissue Eng Part B Rev* 18:167–180.
- Isaacson BM, Bloebaum RD. 2010. Bone bioelectricity: what have we learned in the past 160 years? *J Biomed Mater Res A* 95:1270–1279.
- Merrill DR, Bikson M, Jefferys JG. 2005. Electrical stimulation of excitable tissue: design of efficacious and safe protocols. *J Neurosci Methods* 141:171–198.
- Hronik-Tupaj M, Rice WL, Cronin-Golomb M, et al. 2011. Osteoblastic differentiation and stress response of human mesenchymal stem cells exposed to alternating current electric fields. *Biomed Eng Online* 10:1–22.
- Pedrotty DM, Koh J, Davis BH, et al. 2005. Engineering skeletal myoblasts: roles of three-dimensional culture and electrical stimulation. *Am J Physiol Heart Circ Physiol* 288: H1620–H1626.
- Tandon N, Cannizzaro C, Figallo E, et al. 2006. Characterization of electrical stimulation electrodes for cardiac tissue engineering. *Conf Proc IEEE Eng Med Biol Soc* 1:845–848.
- Kim IS, Song JK, Zhang YL, et al. 2006. Biphasic electric current stimulates proliferation and induces VEGF production in osteoblasts. *Biochim Biophys Acta* 1763:907–916.
- Nuccitelli R. 2003. A role for endogenous electric fields in wound healing. *Curr Top Dev Biol* 58:1–26.
- Titushkin I, Cho M. 2009. Regulation of cell cytoskeleton and membrane mechanics by electric field: role of linker proteins. *Biophys J* 96:717–728.
- Kim IS, Song JK, Song YM, et al. 2009. Novel effect of biphasic electric current on in vitro osteogenesis and cytokine production in human mesenchymal stromal cells. *Tissue Eng Part A* 15:2411–2422.
- Kim IS, Song JK, Song YM, et al. 2008. Novel action of biphasic electric current in vitro osteogenesis of human bone marrow mesenchymal stromal cells coupled with VEGF production. *Bone* 43:S43–S44.
- McCaig CD, Rajnicek AM, Song B, et al. 2005. Controlling cell behavior electrically: current views and future potential. *Physiol Rev* 85:943–978.
- Brighton CT, Wang W, Seldes R, et al. 2001. Signal transduction in electrically stimulated bone cells. *J Bone Joint Surg Am* 83-A:1514–1523.
- Bodamyali T, Bhatt B, Hughes FJ, et al. 1998. Pulsed electromagnetic fields simultaneously induce osteogenesis and upregulate transcription of bone morphogenetic proteins 2 and 4 in rat osteoblasts in vitro. *Biochem Biophys Res Commun* 250:458–461.
- Fassina L, Visai L, Benazzo F, et al. 2006. Effects of electromagnetic stimulation on calcified matrix production by SAOS-2 cells over a polyurethane porous scaffold. *Tissue Eng* 12:1985–1999.
- Lohmann CH, Schwartz Z, Liu Y, et al. 2003. Pulsed electromagnetic fields affect phenotype and connexin 43 protein expression in MLO-Y4 osteocyte-like cells and ROS 17/2.8 osteoblast-like cells. *J Orthop Res* 21:326–334.
- Vander Molen MA, Donahue HJ, Rubin CT, et al. 2000. Osteoblastic networks with deficient coupling: differential effects of magnetic and electric field exposure. *Bone* 27:227–231.
- Sundelacruz S, Li C, Choi YJ, et al. 2013. Bioelectric modulation of wound healing in a 3D in vitro model of tissue-engineered bone. *Biomaterials* 34:6695–6705.

28. Bhumiratana S, Grayson WL, Castaneda A, et al. 2004. Nucleation and growth of mineralized bone matrix on silk-hydroxyapatite composite scaffolds. *Biomaterials* 32: 2812–2820.
29. Nazarov R, Jin HJ, Kaplan DL. 2004. Porous 3-D scaffolds from regenerated silk fibroin. *Biomacromolecules* 5:718–726.
30. Sofia S, McCarthy MB, Gronowicz G, et al. 2001. Functionalized silk-based biomaterials for bone formation. *J Biomed Mater Res* 54:139–148.
31. Altman GH, Horan RL, Martin I, et al. 2002. Cell differentiation by mechanical stress. *FASEB J* 16:270–272.
32. Wang W, Wang Z, Zhang G, et al. 2004. Up-regulation of chondrocyte matrix genes and products by electric fields. *Clin Orthop Relat Res* 427:163–173.
33. Brighton CT, Wang W, Clark CC. 2006. Up-regulation of matrix in bovine articular cartilage explants by electric fields. *Biochem Biophys Res Commun* 342:556–561.
34. Clark CC, Wang W, Brighton CT. 2014. Up-regulation of expression of selected genes in human bone cells with specific capacitively coupled electric fields. *J Orthop Res* 32:894–903.
35. Ercan B, Webster TJ. 2010. The effect of biphasic electrical stimulation on osteoblast function at anodized nanotubular titanium surfaces. *Biomaterials* 31:3684–3693.
36. Huczynski A, Janczak J, Lowicki D, et al. 2012. Monensin A acid complexes as a model of electrogenic transport of sodium cation. *Biochim Biophys Acta* 1818:2108–2119.
37. Serrano-Martin X, Payares G, Mendoza-Leon A. 2006. Glibenclamide, a blocker of K⁺(ATP) channels, shows anti-leishmanial activity in experimental murine cutaneous leishmaniasis. *Antimicrob Agents Chemother* 50:4214–4216.
38. Levin M. 2007. Large-scale biophysics: ion flows and regeneration. *Trends Cell Biol* 17:261–270.
39. Manjubala I, Woesz A, Pilz C, et al. 2005. Biomimetic mineral-organic composite scaffolds with controlled internal architecture. *J Mater Sci Mater Med* 16:1111–1119.
40. Datta N, Holtorf HL, Sikavitsas VI, et al. 2005. Effect of bone extracellular matrix synthesized in vitro on the osteoblastic differentiation of marrow stromal cells. *Biomaterials* 26:971–977.
41. Marom R, Shur I, Solomon R, et al. 2005. Characterization of adhesion and differentiation markers of osteogenic marrow stromal cells. *J Cell Physiol* 202:41–48.
42. Berge U, Kristensen P, Rattan SI. 2008. Hormetic modulation of differentiation of normal human epidermal keratinocytes undergoing replicative senescence in vitro. *Exp Gerontol* 43:658–662.
43. Gong B, Asimakis GK, Chen Z, et al. 2006. Whole-body hyperthermia induces up-regulation of vascular endothelial growth factor accompanied by neovascularization in cardiac tissue. *Life Sci* 79:1781–1788.
44. Shui C, Scutt A. 2001. Mild heat shock induces proliferation, alkaline phosphatase activity, and mineralization in human bone marrow stromal cells and Mg-63 cells in vitro. *J Bone Miner Res* 16:731–741.
45. Morimoto RI. 1993. Cells in stress: transcriptional activation of heat shock genes. *Science* 259:1409–1410.
46. Yamazaki Y, Sejima H, Yuguchi M, et al. 2007. Cellular origin of microfibrils explored by monensin-induced perturbation of secretory activity in embryonic primary cultures. *J Oral* 49:107–114.
47. Moreau R, Aubin R, Lapointe JY, et al. 1997. Pharmacological and biochemical evidence for the regulation of osteocalcin secretion by potassium channels in human osteoblast-like MG-63 cells. *J Bone Miner Res* 12:1984–1992.
48. Bowler WB, Buckley KA, Gartland A, et al. 2001. Extracellular nucleotide signaling: a mechanism for integrating local and systemic responses in the activation of bone remodeling. *Bone* 28:507–512.
49. Orriss IR, Key ML, Hajjawi MO, et al. 2013. Extracellular ATP released by osteoblasts is a key local inhibitor of bone mineralisation. *PLoS ONE* 8:1–13.
50. Wiesmann H, Hartig M, Stratmann U, et al. 2001. Electrical stimulation influences mineral formation of osteoblast-like cells in vitro. *Biochim Biophys Acta* 1538:28–37.

SUPPORTING INFORMATION

Additional supporting information may be found in the online version of this article at the publisher's web-site.